Nanoscale Horizons

ROYAL SOCIETY OF CHEMISTRY

REVIEW

View Article Online
View Journal | View Issue

Cite this: *Nanoscale Horiz.*, 2025, **10**, 1802

Nucleic acid-based chiral nanostructures and their biomedical applications

Shuhui Yu,†[ad] Yiming Xie,†[bd] Yunfei Jiao,[cd] Na Li*[cd] and Baoquan Ding *[abcd]

Chirality is a universal phenomenon in nature. Chiral structures refer to two objects that are mirror images and cannot be superimposed on each other by any kind of translation or rotation. Nucleic acids, including DNA and RNA, are chiral structures. Different chiral geometries of nucleic acids, such as A-form, B-form, and Z-form DNA, and mirror L-nucleic acids, have different properties and physiological functions. This review covers the fundamentals and recent progress in nucleic acid-based chiral nanostructures and their biomedical applications. We begin by introducing chiral geometries of nucleic acids, including naturally occurring A-form, B-form, and Z-form DNA, and artificially synthesized mirror L-nucleic acids. Then the recent advances in creating chiral nanostructures using nucleic acids themselves are presented in the following part. In particular, we highlight the emerging biomedical applications of nucleic acid-based chiral nanostructures. Finally, in the Conclusion section, we provide our views on future challenges and prospects of nucleic acid-based chiral nanostructures.

Received 11th March 2025,
Accepted 5th June 2025

DOI: 10.1039/d5nh00140d

rsc.li/nanoscale-horizons

Introduction

Chiral phenomena are ubiquitous in nature from macroscopic to microscopic scales. Chirality is of significance for the development of novel biomaterials and manifests great potential in various biomedical applications. Nucleic acids, as carriers of genetic information, have important physiological functions and are essential for life processes. Double-strand DNA is usually in A-form, B-form, and Z-form structure and double-strand RNA is usually in A-form structure. Since the development of chemical synthesis of nucleic acids, nucleic acids with mirror chirality (L-DNA or L-RNA) can be synthesized to possess the same informational capacity but are resistant to biodegradation, and may serve as bioorthogonal information repositories or robust drug delivery systems. Moreover, Z-form DNA or mirror L-nucleic acid nanostructures offer unprecedented flexibility in structural design and provide unique physiological properties that have potential applications in biomedicine.

In this review, we introduce the chiral geometries of nucleic acids and the chiral nanostructures constructed by nucleic acids themselves. We further discuss the potential applications of nucleic acid-based chiral nanostructures in biomedicines. Finally, we conclude this review with our views on the future challenges and perspectives of nucleic acid-based chiral nanostructures, and look forward to providing the enlightenment for researchers interested to this field.

The chirality of nucleic acids

The natural chirality of nucleic acids

Nucleic acid is the general term for DNA and RNA. Deoxynucleotides are the basic building blocks of DNA and contain four bases: adenine (A), thymine (T), cytosine (C), and guanine (G). The basic unit of RNA is ribonucleotide, which also contains four bases, but thymine (T) is replaced by uracil (U). The chirality of nucleic acids is different due to the asymmetry of the composition of deoxyribose or ribose sugars that make up the DNA or RNA backbone. Among them, DNA has a variety of configurations, and different configurations of DNA play different roles.[1] The most common configuration of DNA is the right-handed B-form double helix structure, with 10.5 base pairs per rotation (Fig. 1(A)). B-form DNA is often used as a storage of genetic information, and participates in the transcription and replication process. A-form DNA is also a right-handed helix structure (Fig. 1(A)), which usually occurs when DNA is paired with RNA, and it is shorter and thicker than B-DNA. The researchers found that the A-DNA may play a role in the clover structure of tRNA.[2] Z-form DNA, *i.e.* Z-DNA, was discovered by Rich *et al.* with a left-handed double helix

[a] *Henan Institutes of Advanced Technology, Zhengzhou University, Zhengzhou, 450001, China. E-mail: dingbq@nanoctr.cn*
[b] *School of Materials Science and Engineering, Zhengzhou University, Zhengzhou, 450001, China*
[c] *University of Chinese Academy of Sciences, Beijing 100049, China. E-mail: lin@nanoctr.cn*
[d] *Laboratory of Nanosystem and Hierarchical Fabrication, CAS Center for Excellence in Nanoscience, National Center for Nanoscience and Technology, Beijing, 100190, China*
† These authors contributed equally to this work.

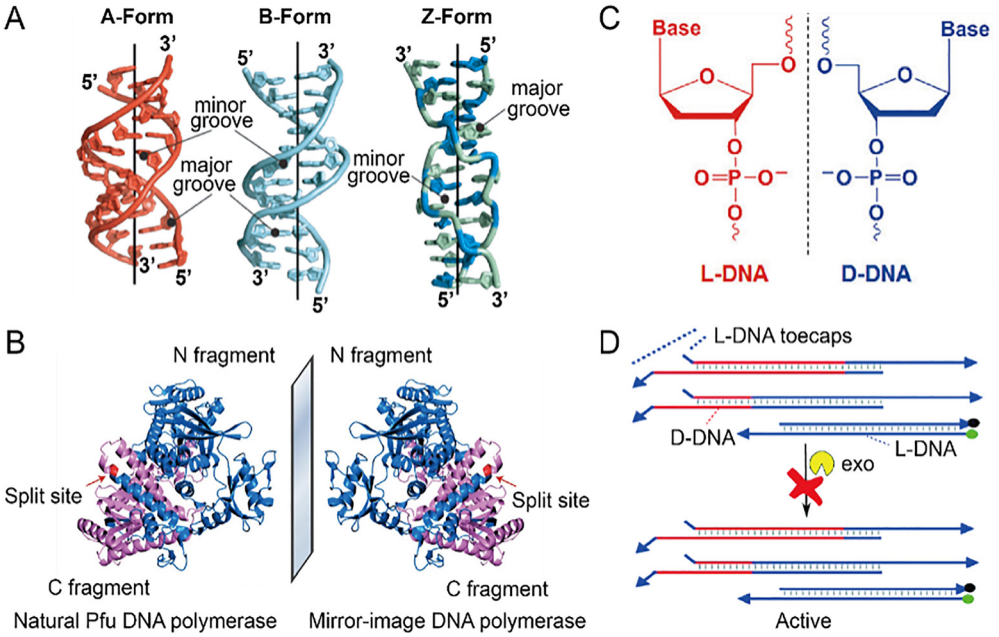

Fig. 1 Different geometries of nucleic acids. (A) Different geometries of DNA. Reproduced with permission.[12] Copyright 2023, Multidisciplinary Digital Publishing Institute. (B) The natural and the synthetic mirror-image Pfu DNA polymerases. Reproduced with permission.[20] Copyright 2021, The Author(s) (C) The structure of L-DNA and D-DNA. Reproduced with permission.[23] Copyright 2012, American Chemical Society (D) Resistance of L-DNA toecaps to exonuclease degradation. Reproduced with permission.[25] Copyright 2022, American Chemical Society.

structure in 1979.[3] Its molecular skeleton is zigzag, hence named Z-DNA (Fig. 1(A)). With the discovery of proteins that can recognize left-handed helix, the functions and biological applications of left-handed nucleic acids are being widely studied.[4] Huang and Zhang *et al.* found that the formation of Z-DNA was affected by chromatin remodeling.[5] In addition, the formation of Z-DNA is also affected by the mechanical properties of DNA. Lee *et al.* found that DNA bending promoted the transition from B-DNA to Z-DNA under physiological salt conditions by regulating the bending force of double strands (ds) DNA.[6] Zhao *et al.* found that endogenous polyamines can induce the conversion of B-DNA to Z-DNA, reducing the affinity for cyclic GMP-AMP synthase (cGAS).[7] The role of Z-DNA in organisms also has been extensively studied. Pasparakis *et al.* investigated the biological functions of Z-DNA and Z-RNA and found that they could trigger RIPK3-dependent cell death and inflammatory responses through Z-DNA binding protein 1 (ZBP1).[8] Rich *et al.* identified that left-handed helical Z-DNA could bind to the Zα domain of adenosine deaminase acting on RNA1 (ADAR1) through contact with a "zigzag"-type sugar-phosphate backbone, which helped to reveal the role of Z-DNA in biological processes.[9] In addition, Z-DNA is also related to the formation of biofilms. As the biofilm matures, Z-DNA accumulates and provides structural integrity to the biofilm matrix through the stabilizing action of the DNABII protein.[10]

Unlike the double-stranded structure of DNA, most RNA molecules are usually single-stranded and can be folded into complex three-dimensional (3D) structures. It is only in certain special cases that RNA can form a local double helix. RNA is commonly formed in A-form RNA with the right-handed helix, and has 11 base pairs per rotation.[11] Z-RNA is an uncommon RNA configuration, and has a left-handed double helix structure, which is similar to Z-DNA (Fig. 1(A)).[12] Its ribose-phosphate backbone is also arranged in a "z" shape, but this unusual RNA configuration is only formed under certain conditions, such as high salt concentrations or in the presence of certain sequences.[13] Z-RNA has been found to exist in both prokaryotic cells[14] and eukaryotic cells.[15] Z-RNA also plays an important role in living organisms. For instance, influenza viruses can produce Z-RNA during replication, which activates the ZBP1 protein in the host, initiating a series of molecular events that lead to cell necrosis.[16]

The mirror-image L-nucleic acids

Pasteur first proposed the concept of a mirror-image world of biology soon after he discovered molecular chirality more than 160 years ago.[17] Such mirror-image biology systems require chirality-inverted enzymes and substrates involved in the central dogma of molecular biology.[18,19] Zhu *et al.* proposed a strategy to synthesize long L-nucleic acid molecules through enzymatic polymerization by mirror-image polymerases (Fig. 1(B)).[20] They chemically synthesize a 90-kDa high-fidelity mirror-image Pfu DNA polymerase that enables accurate assembly of a kilobase-sized mirror-image gene. Apart from mirror-image DNA polymerase, Sczepanski *et al.* developed a cross-chiral RNA polymerase using *in vitro* evolution starting from a population of random-sequence RNAs.[21] Such cross-chiral RNA polymerase could catalyse the joining of L-mono- or oligonucleotide substrates on a complementary L-RNA template, avoiding the chiral inhibition. The activity of cross-chiral RNA polymerase was proved to sufficiently generate full-length copies of its enantiomer through the templated joining

of 11 component oligonucleotides, enabling RNA replication and RNA-based evolution to occur. Their work opens opportunities for constructing advanced mirror-image biology systems and expanding the applications in biotechnology and biomedicine.

As another left-handed structure of DNA, the mirror-image L-DNA has the higher stability than its counterpart D-DNA, because it is more resistant to nuclease degradation (Fig. 1(C)).[22,23] In 1996, Fürste *et al.* discovered mirror-image selection process for the generation of biostable L-oligonucleotides. This breakthrough work lays the foundation for the following biomedical application of L-oligonucleotides.[24] Lakin *et al.* used the L-DNA domain as a protective cap to address the issue of easy degradation of D-DNA in serum (Fig. 1(D)).[25] Sczepanski *et al.* constructed a biostable base excision repair (BER) probe using a unique chimeric D/L-DNA architecture.[26] This chimeric probe, in which the target D-DNA was embedded into L-DNA, exhibited excellent stability in both serum and living cells, and can be used for real-time monitoring of BER activity in living cells. Toehold-mediated strand-displacement has been proven to be a powerful tool for programming DNA-based circuits or nanodevices that are capable of complex logic functions.[27,28] Previously reported heterochiral strand-displacement reactions relied on peptide nucleic acid (PNA) until Sczepanski's work emerged.[29] Sczepanski *et al.* successfully utilized chimeric D/L-DNA complexes to realize heterochiral strand displacement in the absence of PNA.[30] The chimeric D/L-DNA complex allows a homochiral strand-displacement reaction between a D-DNA input and the D-DNA sequence domains that trigger the melting and release of the L-DNA sequence domain from the same complex (or *vice versa*). *Via* this way, it effectively yields an output strand (or sequence domains) having the opposite chirality as the input. Importantly, the heterochiral strand displacement based on the chimeric D/L-DNA complexes can be engineered in harsh biological environments and is compatible with RNA inputs. In addition, Ewers *et al.* investigated the performance of DNA points accumulation for imaging in nanoscale topography (DNA-PAINT) between left-handed (L-) and right-handed (D-) DNA-PAINT. They found that replacing D-DNA-PAINT with L-DNA-PAINT could reduce the interference with the imaging signal, because L-DNA-PAINT could not hybridize to naturally occurring D-DNA.[31]

The chiral nanostructures constructed by nucleic acids

Researchers have begun to explore the use of nucleic acids in the fabrication of various well-defined chiral nanostructures ranging from nanometers to sub-micrometers. The programmable self-assembly of chiral nanostructures constructed by multiple nanoparticles with the assistant of DNA molecules or DNA nanostructures is an important field. Many excellent reviews have summarized the recent progress on this subject,[32–35] and the interested readers are referred to those literatures. Instead, this section emphasizes chiral nanostructures constructed by nucleic acids themselves.

Z-DNA has been shown to form a left-handed duplex *in vivo* and regulate the expression of the corresponding gene. However, it is hard to obtain the stable Z-DNA *in vitro* under normal physiological conditions, mainly because Z-DNA is easily converted to the thermodynamically favorable B-DNA. The stable Z-DNA was usually obtained under high salt conditions, limited sequences, ancillary additives, or chemical modifications. However, An and Liang *et al.* presented a method to construct the stable Z-DNA under normal physiological conditions simply by mixing two complementary minicircles of single-stranded DNA with no chemical modification, due to the topological constraint induced by the hybridization of the minicircles (Fig. 2(A)).[36] Moreover, Liang's group demonstrated that the left-handed duplex part of stable Z-DNA can be generated for various sequences by hybridization of two complementary short circular ssDNAs due to the strong topological constraint.[37] They further constructed an LR-chimera (involving a left-handed part and a right-handed one) with an ssDNA loop by the hybridization of a larger circular ssDNA with a smaller circular ssDNA (Fig. 2(B)).[38] They demonstrated that formed Z-DNA with the extra ssDNA loop is also stable under physiological ionic conditions. The ssDNA loop on the LR-chimera can be used to attach other molecules by hybridization for various potential applications, such as bio-/chemical sensing, diagnosis, or disease treatment. In 1999, Seeman *et al.* constructed a B–Z switchable DNA molecular machine.[39] They constructed a supramolecular device consisting of two rigid DNA 'double-crossover' (DX) molecules connected by 4.5 double-helical turns, which is a 20-nucleotide region of proto-Z DNA in the B-DNA conformation. B $\pm$ Z transition takes place at high ionic strength, where a proto-Z sequence converted to left-handed Z-DNA. This small DNA system provides the possibility of preparing a variety of complex nanomechanical motions.

The use of L-DNA as a backbone for the construction of chiral DNA nanostructures demonstrates superior stability over the natural D-DNA backbone. Liu's group reported the first thermally stable and pH-responsive quadruplex intercalated motif (i-motif) structure fabricated by L-DNA (Fig. 2(C)).[40] Such L-type i-motif exhibits the same physiochemical properties as its D-isomer, but shows inverted chirality and good enzymatic resistance. Subsequently, the same group used L-DNA instead of D-DNA to self-assemble L-DNA hydrogels, which not only inherited the extraordinary physical properties of D-DNA hydrogels, but also exhibited high biological stability and low *in vitro* inflammatory responses (Fig. 2(D)).[41]

Due to the programmable nature of DNA molecules, the self-assembly of DNA molecules can be used to create complex 3D chiral shapes through precise design. Shih *et al.* controlled the twisting and bending of DNA bundles by purposefully inserting and deleting base pairs, resulting in overall left- or right-handed distortion and curvature morphologies at the macroscopic level (Fig. 2(E)).[42] Furthermore, Sun *et al.* investigated a method to program the width of the DNA helix tube by controlling the stiffness and curvature of the repeating unit.[43] By adjusting the twisting density of the cuboid elements with different layers, spiral tubes with different diameters and

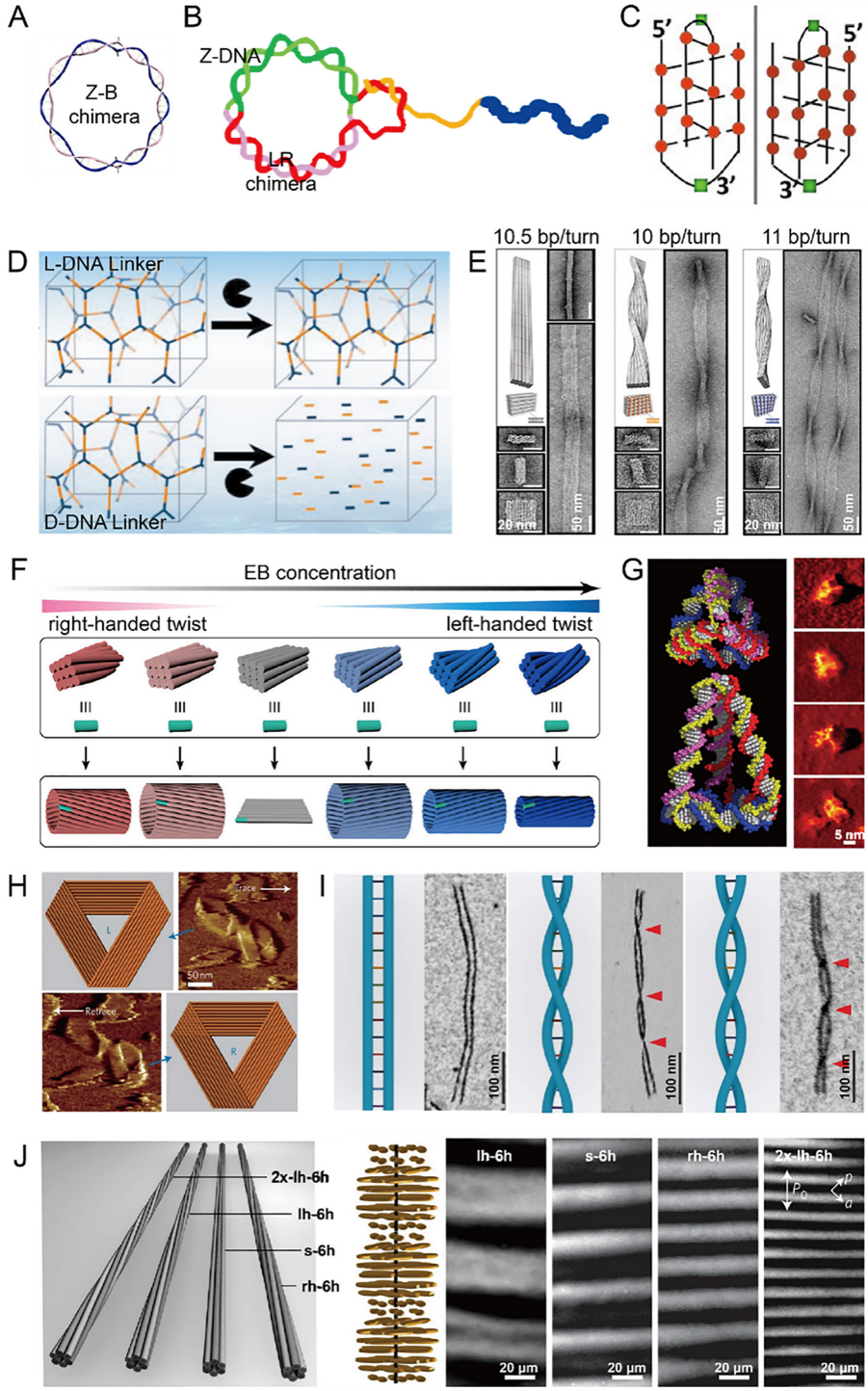

Fig. 2 Various chiral DNA nanostructures. (A) Z-DNA formed in the left half as a chimera hybrid with B-DNA (Z–B chimera) simply by mixing two complementary ssDNA circles. Reproduced with permission.[36] Copyright 2019, American Chemical Society (B) LR-chimera involving non-modified Z-DNA attaching to a variety of molecules. Reproduced with permission.[38] Copyright 2022, the authors (C) The quadruplex intercalated motif (i-motif) structure fabricated by L-DNA. Reproduced with permission.[40] Copyright 2019 Wiley-VCH Verlag GmbH & Co. KGaA, Weinheim (D) The DNA hydrogels constructed by L-DNA and D-DNA linkers. Reproduced with permission.[41] Copyright 2022, Wiley-VCH Gmb. (E) Different chiral band models formed by different twin spiral twist densities. Reproduced with permission.[42] Copyright 2009, Science. (F) The assembling diverse nanotubes from identical DNA tiles with the assistance of EB. Reproduced with permission.[44] Copyright 2024, American Chemical Society (G) Design and AFM images of diastereomeric DNA tetrahedron. Reproduced with permission.[50] Copyright 2005, American Association for the Advancement of Science Reproduced with permission. (H) Co-existence of both left-handed and right-handed chiral Möbius DNA strips. Reproduced with permission.[53] Copyright 1969, Springer Nature (I) Double-stranded *meta*-DNA that can be created as right-handed or left-handed structures. Reproduced with permission.[54] Copyright 2020, The Author(s) (J) Schematics and polarization micrograph of cholesteric liquid crystalline samples comprised of four different DNA origami filaments with varying twists along the filament's long axis. Reproduced with permission.[55] Copyright 2017, Springer Nature.

chiralities were constructed. These DNA helical tubes with specific diameters and chirality can serve as good platforms for the construction of more complex nanostructures or biosensors. Recently, Pan *et al.* reported an intercalator-assisted DNA tile assembly method allowing for assembling DNA nanotubes featuring various widths and chirality using identical DNA strands (Fig. 2(F)).[44] The presence of intercalators like ethidium bromide (EB) tends to drive the right-handed DNA tiles into left-handed twisted conformation. The twisting direction and extent of the DNA tiles could be controlled by varying the concentration of intercalators. Turberfield *et al.* designed and constructed DNA nanotubes of different chiralities by assembly of 2D DNA arrays with 'double-crossover' (DX) DNA tiles along different basis vectors of the DX lattice.[45] These DNA arrays have curled and closed on themselves to form tubes with helical order. The resulting DNA nanotubes possess both the intrinsic chirality of the DNA molecules and an additional mesoscopic chirality arising from the chosen basis vector. Liedl *et al.* produced DNA helical nanotubes of defined chirality by introducing discrete amounts of bending and twist through base pair insertions and/or deletions.[46] The DNA helical nanotubes can be widely controlled with the helical diameters ranging from tens of nanometers to a few micrometers. Moreover, Liu and Yan *et al.* reported the facile preparation of designer discrete or periodic chiral nanostructures, such as four-arm junction structures, nanotubes, 2D nanoarrays using mirror-image L-DNA, and the natural D-DNA.[47] L-DNA and D-DNA possess the same duplex conformation except for their opposite chirality.[48,49] Turberfield *et al.* demonstrated a method for rapid chiral assembly of a family of DNA tetrahedron diastereomers (Fig. 2(G)).[50] They assembled one regular and nine different irregular tetrahedra *via* programmable DNA linkers. The yields of a single diastereomer can reach up to 95%. Mao's group reported a well-defined 3D chiral DNA octahedra by using an unsymmetrical cross motif located at the vertices of DNA octahedra.[51] Following this work, they successfully constructed DNA triangular prisms by using asymmetric DNA three-point-star motifs, and further realized the control of the chirality of DNA nanocages by tuning the angles at the DNA junctions.[52]

DNA origami can also be used to construct chiral nanostructures. Yan *et al.* engineered various types of DNA origami nanostructures to fabricate left- and right-handed Möbius strips (Fig. 2(H)).[53] They showed that the DNA Möbius strip can be reconfigured through strand displacement to create supercoiled ring and catenane structures. Their work may generate unique topological nanostructures with novel material properties by further self-assembly with other materials. Fan and Yan *et al.* developed a *meta*-DNA strategy that a six-helix bundle DNA origami nanostructure in the submicrometer scale (*meta*-DNA) that could be used as a magnified analogue of ssDNA (Fig. 2(I)).[54] Two *meta*-DNAs that contain complementary '*meta*-base pairs' can form double helices with programmed handedness and helical pitches. The right-handed double-stranded *meta*-DNA was found to be almost five times more rigid than its left-handed counterpart. It suggests that chirality plays an important role in the mechanical properties of such structures. They also constructed a series of DNA architectures on a submicrometer-to-micrometer scale using *meta*-DNA strategy, and their strategy provides a promising way to scale up the size of DNA nanostructures.

The sufficiently high densities of DNA chiral molecules provide the opportunity to break the symmetry of the underlying molecular interactions, which manifests them the long-range chiral order, known as a chiral nematic liquid crystal (LC) phase or cholesteric phase. The chiral properties of cholesteric phase varied between long and short DNA strands (Fig. 2(J)).[55] Long DNA helices generally tend to yield a left-handed cholesteric phase. However, short DNA with base pairs between 8 and 20 bp can form both right- and left-handed cholesteric arrangements. The handedness of DNA cholesterics depends on several parameters, such as the length, the sequence, and the concentration of oligonucleotide. A high concentration of oligonucleotide is generally prone to produce a right-handed LC, and the critical concentration for handedness inversion corresponds to the inter-helical distances close to the helical pitch. DNA origami technology provides a rapid and robust platform for constructing chiral LC. Dietz and Dogic *et al.* reported cholesteric LCs fabricated by DNA origami filaments (Fig. 2(K)).[56] The designable and programmable DNA origami technology offers a powerful tool to exquisitely control the microscopic filament structure and finetune the macroscopic cholesteric pitch. The bundles of DNA were programmed to have different amounts of twist, varying from left-handed to neutral and to right-handed. The tunable macroscopic chirality of the LC phases could be obtained by mixing two DNA filaments with opposite chirality. Their work could be extended to synthesize DNA-based chiral plasmonic nanostructures with unprecedented photonic properties. In addition, Tortora *et al.* theoretically analyzed the mechanism of chirality amplification in lyotropic LCs, and elucidated the influence of DNA intramolecular mechanics on chiral supramolecular order.[57] Their work provided a systematic study of the relationship between molecular interactions and cholesteric behavior. In addition, Che *et al.* reported the first example of DNA-silica complex liquid-crystal.[58] The specific effects of cation distribution, silica polymerization, DNA interaxial separation, and DNA-helix orientation render a new DNA liquid-crystal phase system. Furthermore, Che *et al.* have successfully synthesized enantiomeric impeller-like helical DNA-silica complexes by introducing various alkaline earth metal ions into the co-structure-directed synthesis.[59] The induced chiral assembly into nanoscale impeller-like structures with tunable handedness also depends on the pH and temperature of the solution.

The biosensing application of nucleic acid-based chiral nanostructures

DNA molecules have been applied to fabricate chiral materials with subtle chiral nanostructures, which exhibit great potential in bio-/chemical sensing and biological applications. Researchers have developed various biosensors fabricated by chiral DNA molecules or chiral DNA nanostructures with high sensitivity

for detecting and quantifying biomarkers. Given the nuclease-resistance of L-DNA, L-DNA nanostructures can survive in a biological environment, and open up opportunities for a wide range of biomedical applications. For instance, the degradation and interference of the nucleic acid probes in complex biological environments, *e.g.*, cytoplasm or body fluid are the big issues that inevitably cause false-positive signals in biosensing as well as inefficient bioregulation in biomedicine. L-DNA molecular probes, which combine full biocompatibility and resistance to DNase I degradation render them the ideal probes for rapid, accurate, and sensitive sensing. Lyu *et al.* assembled a mirror-image box by L-DNA, termed L-AMBER, to protect encapsulated D-DNA probes from degradation and maintain their responsive activity in complex biological environments (Fig. 3(A)).[60] The L-AMBER probes can resist DNase I degradation compared to the D-AMBER probes, and present low false-positive bioimaging and highly efficient miRNA silence in living cells. Their strategy provides a universal and effective way to enhance the resistance of nucleic acid probes to environmental interference in biosensing and biomedicine applications. DNAzymes refer to single-stranded DNA molecules with catalytic capabilities. A central aspect of DNAzyme activity is the DNAzyme-mediated substrate cleavage with the assistance of metal-ion cofactors.[61] As a result, DNAzyme-based systems are ideal choices for the development of metal ion sensors. Tan and Zhang *et al.* used L-DNAzyme sensor for sensing metal ions in complex biological samples and live cells, and demonstrated that L-DNAzyme possessed similar catalytic activity to that of D-DNAzyme in the presence of the same achiral metal ion cofactors but with the extra merit of biostability in biological matrixes (Fig. 3(B)).[62] Yang *et al.* constructed a special hairpin-structured dual-labeled L-DNA probe.[23] This L-DNA probe relies on the temperature-responsive hairpin structure and the FRET signaling mechanism. The fluorescence of L-DNA probe is quenched below the melting temperature and enhanced with increasing temperature. Importantly, the non-natural L-DNA backbone prevents the L-DNA probe from binding to cellular nucleic acids and proteins as well as from being digested by nucleases inside the cells, thus ensuring excellent stability and accuracy of the nano-thermometer in a complex cellular environment.

Self-assembly of chiral metallic nanostructures has gained significant attention over the past few years due to their tunable chiroptical properties by controlling the size, shape and arrangement of nanoparticles (NPs). DNA molecule is capable of creating customizable chiral metallic nanostructures in a simple and controllable manner. For instance, Xu and Kotov *et al.* fabricated the consistent elongated gold nanorods (AuNRs) 'chains' and 'ladders' by the attachment of AuNRs to each other, followed by either an end-to-end (chains) or a side-by-side (ladders) assembly pattern.[63] Different patterned AuNRs assemblies are controlled by the placement of the PCR primers with the DNA-modified AuNRs, and the number of thermal cycles determines the lengths and complexity of the resulting superstructures. Chirality of 'ladder' assemblies employing different reactant DNA templates can be used for attomolar DNA biosensing. The enhanced sensitivity of this method benefits from the enhancement of polarization rotation by plasmonic structures, chiral symmetry breaking for 'ladders' assemblies, and the bisignate nature of CD spectra. The 'ladders' assemblies have high potential to detect intracellular low-occurrence markers and signaling molecules. Liedl *et al.* created the first three-dimensional (3D) chiral plasmonic metamolecules by DNA origami with tailored optical response.[64] The programmed structural parameters and heterogeneous materials endow chiral metallic nanostructures with the potential for use as a tool in biosensors. Yan *et al.* combined four gold nanoparticles (AuNPs) of the same size by a symmetric DNA frame containing a ssDNA loop on one side to form an achiral pyramid structure (Py1) (Fig. 3(C)).[65] When adding a ssDNA that can hybridize with the DNA loop on Py1, the geometry of the pyramid can transform into an asymmetric reconfigured pyramid (Py2), giving a strong CD signal in the visible region. Furthermore, this CD-based platform can be designed to combine with Ag and AuNPs of different sizes to form a chiral pyramid structure (Py3), which undergoes dissociation into a single heterotrimer through DNA hybridization. It results in the disappearance of the chirality of Py3, and the changes of CD signal simultaneously. The chiroptical response of assemblies is extremely sensitive to configuration changes, and can be used for highly selective and quantitative detection of DNA molecules. Subsequently, Kuang *et al.* assembled an asymmetric dimer in which bisphenol (BPA) aptamer modified on one AuNPs hybridized with their complementary sequences modified on the other AuNP of different sizes.[66] The intensity of the chiral signal of the ensemble was varied under different concentrations of BPA, achieving highly sensitive and selective detection of BPA with no cross-reactivity with BPA analogues.

DNA origami nanostructures can be designed and fabricated the spatially reconfigurable conformation, which are excellent candidates for the custom sensing probes. In 2014, Kuzyk and Liu *et al.* created the first dynamic reconfigurable 3D chiral plasmonic metamolecules by DNA origami.[67] They assembled two AuNRs on a reconfigurable DNA origami template to execute DNA-regulated conformational changes of opened or closed state through toehold-mediated strand displacement reactions on the nanoscale. The configuration of the plasmonic nanostructure could be switched between left-handed, right-handed, and relaxed states. These dynamic plasmonic devices hold great promise for applications in adaptable nanophotonic circuitry, artificial nanomachinery, as well as optical sensing of molecular binding and interaction activities. Huang and Kuzyk *et al.* adopt a similar reconfigurable 3D chiral plasmonic DNA origami structure as a nanosensor for detecting adenosine and adenosine triphosphate, except that the molecular lock was replaced by an adenosine DNA aptamer.[68] The adenosine DNA aptamer as a molecular lock is incorporated into a reconfigurable DNA origami-AuNRs construct and transduces the state of the lock into relaxed configurations of the AuNRs dimer with distinct plasmonic CD responses upon target binding. These aptamer-based sensing platforms can, in principle, be used to

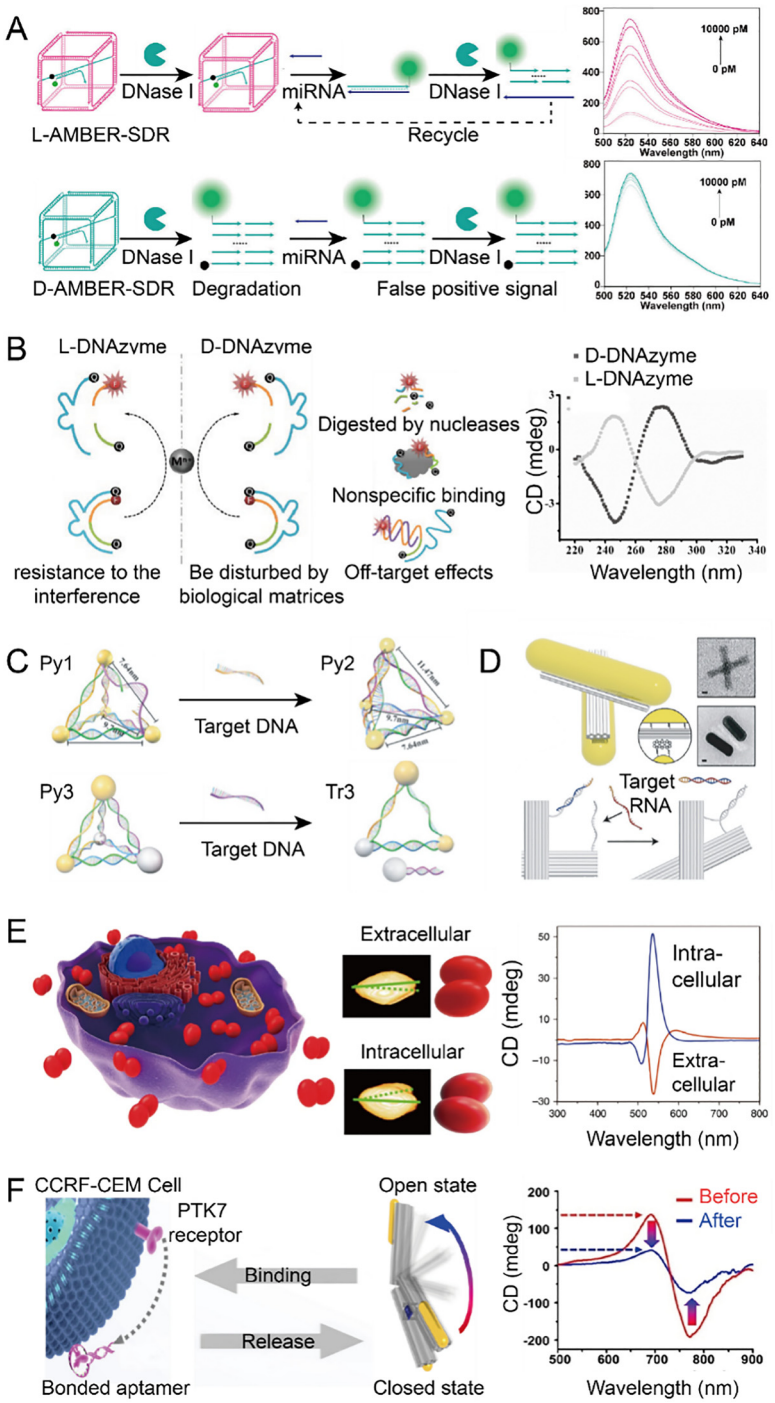

Fig. 3 Nucleic acid-based chiral nanostructures for biosensing. (A) miRNA detection of L-AMBER-SDR and D-AMBER-SDR based on DNase I-assisted signal amplification strategy. Reproduced with permission.[60] Copyright 2024, American Chemical Society (B) L-DNAzyme performs the same function with the help of the same cofactor as D-DNAzyme, and is resistant to the interferences of biological matrixes. Reproduced with permission.[62] Copyright 2015 American Chemical Society (C) Structural changes of the two pyramid DNA nanostructures after hybridizing ssDNA with the DNA loop on Py1 (upper) or releasing a single AgNP from Py3 (lower), resulting in changes in CD signal. Reproduced with permission.[65] Copyright 2024, Wiley-VCH Verlag GmbH & Co. KGaA, Weinhei. (D) A chiral plasmonic switch to sensitively and selectively detect a specific RNA target. Reproduced with permission.[70] Copyright 2018, Wiley-VCH Verlag GmbH & Co. KGaA, Weinheim. (E) CD signaling changes due to AuNPs dimers structural changes when they enter the cells, distinguishing their transmembrane transport process. Reproduced with permission.[74] Copyright 2017, The Author(s). (F) Signal-amplifying DNA nanodevice enhances trace signals into detectable CD responses. Reproduced with permission.[80] Copyright 2022, Wiley-VCH GmbH.

detect a variety of targets of interest based on the specific recognition aptamers. Bae *et al.* adopted dual thrombin aptamers to detect human thrombin proteins based on a similar reconfigurable chiral plasmonic DNA origami structure.[69] The two

different thrombin-binding aptamers were incorporated into each arm of the structure to capture a thrombin molecule. The cooperative binding of the two aptamers exhibited an increasing sensitivity for thrombin protein with an order of magnitude lower Kd (1.4 nM) than that of the individual aptamers. Funck *et al.* fabricated a chiral plasmonic switch to sensitively and selectively detect a specific RNA target (Fig. 3(D)).[70] This chiral plasmonic switch based on a reconfigurable DNA origami template where a chiral arrangement of AuNRs on the structure leads to a strong CD response. Switching of the cross-like DNA structure is achieved by the addition of specific nucleic acid sequences. The specific RNA target binds to a complementary sequence that is part of the lock of the chiral plasmonic switch, resulting in changes in the plasmonic CD spectrum. Therefore, a specific sequence can be detected through the resulting changes in the plasmonic CD spectrum. In addition, Huang and Kuzyk *et al.* developed a competitive hybridization reaction-based strategy for characterizing the affinities and specificities of DNA or RNA aptamers using this reconfigurable chiral plasmonic assemblies.[71,72] This approach relies on a template strand with a fixed sequence and a set of varied complementary strands, both in the hybridization regions and lengths at a fixed analyte concentration. The value of Kd can be obtained by certain equations based on the different CD responses resulting from a single base pair difference in the hybridization of the complementary strand with the template strand. All these works exhibit that reconfigurable chiral plasmonic DNA origami structures are promising candidates as a sensing platform. Cheng *et al.* used the metasurface to enhance the chiral sensing of this reconfigurable 3D chiral plasmonic DNA origami structure.[73] About a 10-fold enhancement of CD response was obtained with the metasurface assistance for the detection of achiral or slightly chiral DNA strands compared with the platform without metasurfaces. Their work presents a high-sensitivity platform for achiral or slightly chiral sensing by the collaborative effect of metasurfaces and reconfigurable chiral plasmonic DNA origami structure. Nucleic acid-based chiral nanostructures can not only be used as biosensors *in vitro*, but also be applied *in vivo* for biosensing, bioimaging, or disease diagnosis. Kuang and Kotov *et al.* fabricated DNA-bridged AuNPs dimers which can be used to monitor the internalization process of particles by the mammalian cells in real time and distinguish the localization inside and outside cells (Fig. 3(E)).[74] The nanoparticle dimers changed from a right-handed to a left-handed configuration and the CD signal changes from negative to positive when they entered the cell, distinguishing their transmembrane transport process. Kuang and Liz-Marzán *et al.* described the intracellular chiral assembly of AuNRs dimers for the spatially resolved detection of intracellular miRNA.[75] The selective recognition of specific miRNA sequences by ssDNA bounded to Au NRs would induce the formation of twisted side-by-side (SBS) dimers, which display circular dichroism (CD) in the visible and near-infrared spectral range. Their strategy can be used for *in situ* imaging and semiquantification of target biomarkers. Upconversion nanoparticles (UCNPs) are a special class of luminescence nanomaterials that are capable of converting low-energy light (*e.g.*, near-infrared light) into high-energy light (*e.g.*, visible light). UCNPs are considered nontoxic, and have a narrower band emission and longer fluorescence lifetime, which have made them promising luminescent materials in the biomedical field.[76,77] Kuang *et al.* designed a propeller-shaped AuNR-UCNP tetramer with strong chiral activity and upconversion luminescence which can overcome the problem of low luminescence efficiency of traditional luminescent materials. Meanwhile, the chiral geometry of such systems also enables DNA detection with an unusually low limit of detection,[78] showing potential for efficient bioimaging, early medical diagnosis, environmental monitoring, and fingerprint forensics. Kuang *et al.* constructed a DNA-driven Au-UCNP pyramid structure as an intracellular nanoprobe for the ultrasensitive and selective detection of miRNA in living cells.[79] The Au-UCNP pyramids display both strong plasmonic CD and significant luminescence, and therefore can be monitored by dual plasmonic CD and luminescent signals. The target miRNA will be integrated with the recognition sequence on the DNA framework, resulting in the dissociation of the DNA framework. The disintegration of the pyramid structure resulted in the attenuation of the CD signal and the increased fluorescence intensity of UCNPs which enables the detection of miRNAs. This approach opens up a new avenue to the ultrasensitive detection and *in situ* quantification of miRNA in living cells. Ding and Jiang *et al.* designed and fabricated a signal-amplified DNA origami nanodevice based on DNA circuit-assisted chiral plasmonic nanosystem (Fig. 3(F)).[80] In this system, two AuNRs are co-assembled onto a tweezer-like DNA origami template containing DNA lock to form the chiral plasmonic nanostructure. The input signals, such as nucleic acids, adenosines, chiral tyrosinamides or specific receptors expressed by tumor cells could activate the plasmonic nanodevices and produce DNA keys for opening the DNA lock. Then this system undergoes the cascade amplification process to drive conformational changes in the plasmonic nanodevices, reporting robust responses *via* CD spectral changes. This signal-amplifying DNA nanodevice will be manipulated to enhance trace signals into detectable CD responses.

The nucleic acid-based chiral nanostructures for disease surveillance or treatment

The nucleic acids of different configurations have their own division of labor and play an irreplaceable role in organisms. Take Z-DNA for example, Mathis *et al.* found that the formation of Z-DNA was associated with the generation of doublet DNA breaks on the promoter of the gene induced by an Autoimmune Regulator (AIRE). AIRE-induced gene expression can be modulated by manipulating the formation of Z-DNA, providing a potential target for the development of new immunomodulatory strategies.[81] Z-form DNA can be recognized by specific reader proteins, such as ADAR1 or ZBP1, to exert downstream biological functions. West *et al.* found that mitochondrial genome instability promotes the accumulation of Z-DNA, while ZBP1 can stabilize Z-mitochondrial DNA and work with cyclic

GMP-AMP synthase (cGAS) to maintain the IFN-I response and promote the development of cardiomyopathy.[82] Later, Bredy *et al.* investigated the effect of Z-DNA binding to ADAR1 on fear memory in mice, and explored the activity-dependent relationship between Z-DNA and ADAR1. They found that Z-DNA bound to ADAR1 reduced Z-DNA levels in fear extinction learning, and demonstrated that Z-DNA binding domain was necessary for memory flexibility.[83] Herbert and Balachandran *et al.* found that endogenous small molecule CBL0137 could potently trigger Z-DNA formation in cells which subsequently activates ZBP1, and induces ZBP1-dependent necroptosis in cancer-associated fibroblasts and reverse immune checkpoint blockade (ICB) unresponsiveness in mouse models of melanoma (Fig. 4(A)).[84] Jin and Wei *et al.* proposed a Z-DNA-based PROTAC (Z-PROTAC) strategy which engaged Z-form DNA with ADAR1 and its degradation is achieved by leveraging a VHL ligand conjugated to Z-form DNA to recruit the E3 ligase (Fig. 4(B)).[85] Selectively degrade the Z-DNA-binding protein

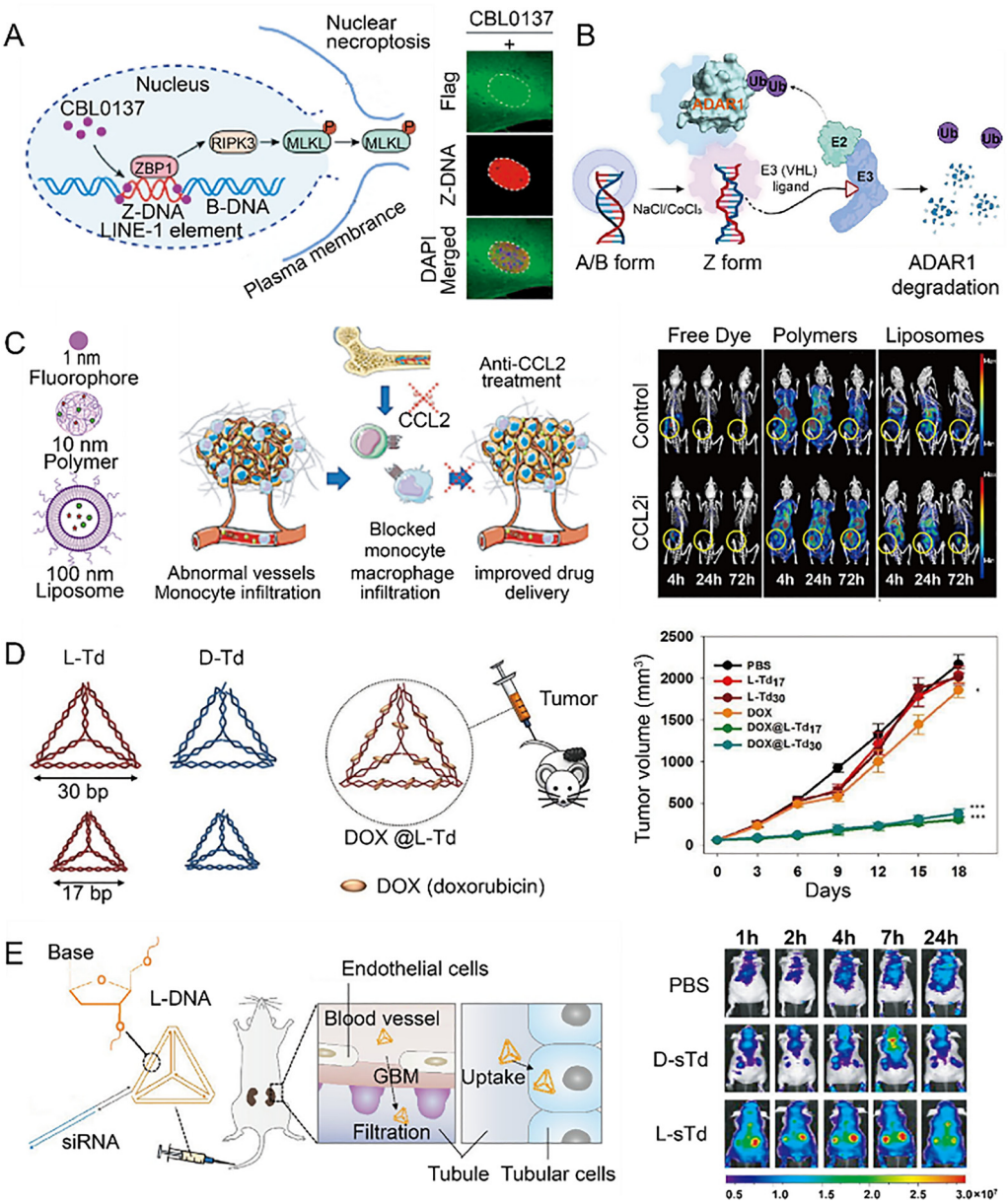

Fig. 4 The nucleic acid-based chiral nanostructures for disease treatment. (A) CBL0137 triggers Z-DNA formation in cells and mediates nuclear necroptosis. Reproduced with permission.[84] Copyright 2022, The Author(s), under exclusive license to Springer Nature Limited. (B) The Z-PROTAC hijacks the VHL E3 ligase for targeted degradation of ADAR1. Reproduced with permission.[85] Copyright 2024, American Chemical Society. (C) L-RNA aptamer NOX-E36 in combination with DOX improves the delivery efficacy of DOX in triple-negative breast cancer by inhibiting the initiation of tumor vasculature. Reproduced with permission.[97] Copyright 2024, Elsevier. (D) L-DNA tetrahedron selectively delivers anti-cancer drug DOX to the tumor site to enhance the anti-cancer effect. Reproduced with permission.[104] Copyright 2016, Elsevier. (E) Specific accumulation of L-DNA tetrahedra in the kidneys for the treatment of acute kidney injury. Reproduced with permission.[107] Copyright 2020, American Chemical Society.

ADAR1 triggers a cascade of PANoptotic events, *e.g.*, apoptosis and necroptosis, by mitigating the blocking effect of ADAR1 on ZBP1, exclusively within cancer cells rather than normal cells. Moreover, Z-PROTAC is proven to elicit a positive immunological response, subsequently leading to a synergistic augmentation of cancer cell death. This structural specificity-induced selective degradation strategy presents the therapeutic landscape both in cancer and immunology.

L-Aptamers are intrinsically resistant to degradation by ribonucleases, and might be an alternative to antisense oligonucleotides to target structured RNAs of biological or therapeutic interest. Joyce *et al.* developed an L-RNA aptamer that binds the natural D-RNA through *in vitro* selection.[86] It is the first example of two nucleic acid molecules of opposing chirality that interact through a mode of binding other than the primary structure. The L-RNA aptamer binds D-RNA exclusively at the six-nucleotide distal loop through tertiary interactions rather than simple Watson–Crick pairing. Nowadays, some aptamers composed of L-DNA and/or L-RNA (so-called Spiegelmer) are widely studied and have great potential in biomedicine.[87] The Spiegelmers were screened by a novel mirror selection scheme investigated by Chen *et al.*[88] This mirror SELEX strategy can select L-DNA aptamers that specifically bind to target molecules from a large randomized L-DNA pool. Spiegelmers are widely studied in basic research. For instance, NOX-L41 and NOX-C89 can be combined with human and mouse calcitonin gene-related peptide (CGRP) to improve primary headache;[89,90] NOX-1255 has a high affinity for gonadotropin-releasing hormone (GnRH), and can be used as an antagonist to GnRH;[91] NOX-A50 in combination with High mobility group A1 (HMGA1) for the treatment of pancreatic cancer;[92] NOX-F37 can bind and inhibit neuropeptide vasopressin (AVP), thereby producing a diuretic effect.[93] The scientists also designed Spiegelmer NOX-D20 with a mixture of L-DNA and L-RNA. NOX-D20 can bind to complement factor C5a, thereby inhibiting C5a-induced chemotaxis in CD88-expressing cell lines and potently antagonizing C5a activation of primary human polymorphonuclear leukocyte (PMN).[94] More importantly, some developed Spiegelmers have currently already been used in clinical practice. For instance, NOX-A12 is a novel Spiegelmer-based SDF-1/CXCL12 antagonist, and SDF-1/CXCL12 is a chemokine involved in the regulation of cell trafficking in chronic lymphocytic leukemia (CLL). NOX-A12 abolishes the protective effect of CXCL12-secreting bone marrow stromal cells (BMSCs) by inhibiting CXCL12.[95] Gobbi *et al.* used NOX-A12 combined with Bortezomib and Dexamethasone for clinical use in patients with recurrent multiple myeloma. They found that NOX-A12 was safe, tolerable, and effective no matter used in a Piecke agent or in combination.[96] NOX-E36 is also a Spiegelmer, which has a high affinity with the inflammatory chemokine CCL2 to block the function of CCL2 and reduce the inflammatory response (Fig. 4(C)).[97] NOX-E36 has been used in clinical practice to treat type 2 diabetes albuminuria and other diseases with good clinical effects.[98] NOX-H94 as another Spiegelmer has been shown to be safe and well tolerated as a hepcidin inhibitor for the treatment of anemia of chronic disease.[99]

L-DNA, the mirror form of natural D-DNA, has thermodynamically identical properties in hybridization.[100–102] Therefore, L-DNA can also be employed as a backbone for the assembly of drug delivery systems. Ahn *et al.* used L-DNA to construct tetrahedral DNA nanocarriers, which showed higher cell uptake and serum stability than D-DNA delivery systems.[103] Based on the advantages of L-DNA nanostructures, L-DNA tetrahedron (L-Td) was subsequently used for tumor-specific delivery of anticancer drugs doxorubicin (DOX) (Fig. 4(D)).[104] L-Td can deliver anticancer drugs DOX selectively to tumors with enhanced cellular and tissue penetration, and show greater anticancer effects *in vitro* and *in vivo* compared with traditional PEGylated liposomes. This work highlights the promising potential of L-DNA nanostructures as a novel drug delivery platform. Furthermore, the same group found that smaller L-Td showed greater potential for enhancing tumor-targeted drug delivery.[105] In addition to use L-Td for the delivery of anticancer drugs, the same group also designed a streptavidin (STV)-Td-based enzyme for intracellular delivery, which can accumulate in tumor tissues and exert therapeutic effects.[106] Various biotinylated enzymes can be loaded onto the STV subunit of the hybrid and systemically delivered to tumor cells through the cell-penetrating and tumor-localizing properties of Td. The hybrid is able to transfer the apoptotic enzyme specifically into tumor cells, leading to strong suppression of tumor growth without causing significant damage to other tissues. These results suggest that the hybrid may allow anti-proliferative enzymes and proteins to be utilized as anticancer drugs. Recently, this L-Tds were developed as a platform for kidney-targeted cytosolic delivery of siRNA (L-sTds, Fig. 4(E)).[107] L-sTds showed obvious kidney-specific accumulation compared to other sTds with different sugar backbone-modified oligonucleotides. The kidney preference and the tubular cell uptake property of L-Tds render L-Tds a promising platform for kidney-targeted intracellular delivery of p53 siRNA to treat acute kidney injury (AKI) in mice.

Conclusions

The chirality of nucleic acids is an intrinsic physical property that exhibits unique functions and shows great potential in applications in both natural form and artificial designs. Moreover, the programmable property of DNA molecules allows the customization of the chiral nanostructures and the functionalities. In this review, we introduced the natural chiral structures of nucleic acids and nucleic acid-based chiral nanostructures. We further summarized the biosensing and biomedicine applications of these chiral materials made from nucleic acids. The nucleic acid-based chiral nanostructures are promising candidates for many biological sensing and biomedicine applications with remarkable target specificity and functionality. However, there is still plenty of room for explorations to further advance the nucleic acid-based chiral nanostructures, and many bottleneck problems still remain and are waiting for solutions.

First of all, the function and regulatory mechanism of nucleic acid chirality in biological systems is still an open

question. For example, how do chiral interactions between different biomolecules and chiral nanostructures affect intracellular signalling and metabolic processes? Moreover, recent work has witnessed the different immune responses *in vitro* and *in vivo* between left- and right-handed nanoparticles or nanostructures.[108] A deeper study of the effect of different chirality in the life course needs to be uncovered to better understand their role in biological systems.

Second, nucleic acid-based chiral nanostructures show great promising potential applications in biomedicine. However, there are still significant gaps between the design and fabrication of nucleic acid-based chiral nanostructures in labs and the practice of those in clinic use. How to apply these chiral nanostructures to solve practical biomedical issues, such as drug delivery, biosensing, and tumor therapies are still hot topics in current and future research. Future work may focus on developing novel composites of nucleic acid-based chiral nanostructures related to specific diseases and more research pipelines are expected for future clinic use.

Third, nucleic acid-based chiral nanostructures may play an important role in the areas such as biocomputing and biorobotics. By programming complex and hierarchical nucleic acid-based chiral nanostructures, rationally designed chiral architectures may be employed as a tool to create high-order computing systems or nanorobotics, which can offer unprecedented opportunities for next-generation information storage or processing.

In summary, nucleic acid-based chiral nanostructure is a multidisciplinary research field, which not only draws much attention in basic scientific research, but also shows great potential in biomedical application. Harnessing chirality of nucleic acid-based nanostructures and deep understanding the intrinsic mechanism between their chiralities and the properties would be benefit for practical applications with marked achievements. As science and technology continue to be developed, more breakthroughs and discoveries of nucleic acid-based chiral nanostructures will be achieved in the future.

Data availability

No primary research results, software or code have been included and no new data were generated or analysed as part of this review.

Conflicts of interest

There are no conflicts to declare.

Acknowledgements

This work was supported by the National Key R&D Program of China National Basic Research Program of China (grant no. 2021YFA1200302), the National Natural Science Foundation of China (grant no. 22025201, 22472041 and 22072033), the Youth Innovation Promotion Association, CAS, and the CAS Project for Young Scientists in Basic Research (grant no. YSBR-036).

Notes and references

1 R. E. Dickerson, H. R. Drew, B. N. Conner, R. M. Wing, A. V. Fratini and M. L. Kopka, *Science*, 1982, **216**, 475–485.
2 S. H. Kim, F. L. Suddath, G. J. Quigley, A. McPherson, J. L. Sussman, A. H. Wang, N. C. Seeman and A. Rich, *Science*, 1974, **185**, 435–440.
3 A. H. Wang, G. J. Quigley, F. J. Kolpak, J. L. Crawford, J. H. van Boom, G. van der Marel and A. Rich, *Nature*, 1979, **282**, 680–686.
4 B. A. Brown, 2nd, K. Lowenhaupt, C. M. Wilbert, E. B. Hanlon and A. Rich, *Proc. Natl. Acad. Sci. U. S. A.*, 2000, **97**, 13532–13536.
5 Y. Li, Q. Huang, G. Yao, X. Wang, F. Zhang, T. Wang, C. Shao, X. Zheng, X. Jing and H. Zhou, *Anal. Chem.*, 2020, **92**, 14452–14458.
6 J. Yi, S. Yeou and N. K. Lee, *J. Am. Chem. Soc.*, 2022, **144**, 13137–13145.
7 C. Zhao, Y. Ma, M. Zhang, X. Gao, W. Liang, Y. Qin, Y. Fu, M. Jia, H. Song, C. Gao and W. Zhao, *Immunity*, 2023, **56**, 2508–2522.
8 H. Jiao, L. Wachsmuth, S. Kumari, R. Schwarzer, J. Lin, R. O. Eren, A. Fisher, R. Lane, G. R. Young, G. Kassiotis, W. J. Kaiser and M. Pasparakis, *Nature*, 2020, **580**, 391–395.
9 T. Schwartz, M. A. Rould, K. Lowenhaupt, A. Herbert and A. Rich, *Science*, 1999, **284**, 1841–1845.
10 J. R. Buzzo, A. Devaraj, E. S. Gloag, J. A. Jurcisek, F. Robledo-Avila, T. Kesler, K. Wilbanks, L. Mashburn-Warren, S. Balu, J. Wickham, L. A. Novotny, P. Stoodley, L. O. Bakaletz and S. D. Goodman, *Cell*, 2021, **184**, 5740–5758.
11 S. Arnott, W. Fuller, A. Hodgson and I. Prutton, *Nature*, 1968, **220**, 561–564.
12 J. B. Krall, P. J. Nichols, M. A. Henen, Q. Vicens and B. Vögeli, *Molecules*, 2023, **28**, 843.
13 K. Hall, P. Cruz, I. Tinoco, T. M. Jovin and J. H. Vandesande, *Nature*, 1984, **311**, 584–586.
14 D. A. Zarling, C. J. Calhoun, C. C. Hardin and A. H. Zarling, *Proc. Natl. Acad. Sci. U. S. A.*, 1987, **84**, 6117–6121.
15 D. A. Zarling, C. J. Calhoun, B. G. Feuerstein and E. P. Sena, *J. Mol. Biol.*, 1990, **211**, 147–160.
16 T. Zhang, C. Yin, D. F. Boyd, G. Quarato, J. P. Ingram, M. Shubina, K. B. Ragan, T. Ishizuka, J. C. Crawford, B. Tummers, D. A. Rodriguez, J. Xue, S. Peri, W. J. Kaiser, C. B. López, Y. Xu, J. W. Upton, P. G. Thomas, D. R. Green and S. Balachandran, *Cell*, 2020, **180**, 1115–1129.
17 L. Pasteur, *Researches on the molecular asymmetry of natural organic products*, University of Hull, 1905, vol. 20, pp. 235–236.
18 Z. Wang, W. Xu, L. Liu and T. F. Zhu, *Nat. Chem.*, 2016, **8**, 698–704.
19 M. Peplow, *Nature*, 2016, **533**, 303–304.
20 C. Fan, Q. Deng and T. F. Zhu, *Nat. Biotechnol.*, 2021, **39**, 1548–1555.

21 J. T. Sczepanski and G. F. Joyce, *Nature*, 2014, **515**, 440–442.
22 X. N. Feng, Y. X. Cui, J. Zhang, A. N. Tang, H. B. Mao and D. M. Kong, *Anal. Chem.*, 2020, **92**, 6470–6477.
23 G. Ke, C. Wang, Y. Ge, N. Zheng, Z. Zhu and C. J. Yang, *J. Am. Chem. Soc.*, 2012, **134**, 18908–18911.
24 A. Nolte, S. Klussmann, R. Bald, V. A. Erdmann and J. P. Fürste, *Nat. Biotechnol.*, 1996, **14**, 1116–1119.
25 T. L. Mallette and M. R. Lakin, *ACS Synth. Biol.*, 2022, **11**, 2222–2228.
26 W. Zhong and J. T. Sczepanski, *J. Am. Chem. Soc.*, 2023, **145**, 17066–17074.
27 F. C. Simmel, B. Yurke and H. R. Singh, *Chem. Rev.*, 2019, **119**, 6326–6369.
28 D. Y. Zhang and G. Seelig, *Nat. Chem.*, 2011, **3**, 103–113.
29 A. M. Kabza, B. E. Young and J. T. Sczepanski, *J. Am. Chem. Soc.*, 2017, **139**, 17715–17718.
30 B. E. Young and J. T. Sczepanski, *ACS Synth. Biol.*, 2019, **8**, 2756–2759.
31 H. J. Geertsema, G. Aimola, V. Fabricius, J. P. Fuerste, B. B. Kaufer and H. Ewers, *Nat. Biotechnol.*, 2021, **39**, 551–554.
32 N. Liu and T. Liedl, *Chem. Rev.*, 2018, **118**, 3032–3053.
33 H. Liu, X. Shen, Z. G. Wang, A. Kuzyk and B. Ding, *Nanoscale*, 2014, **6**, 9331–9338.
34 N. Li, Y. Shang, Z. Han, T. Wang, Z. G. Wang and B. Ding, *ACS Appl. Mater. Interfaces*, 2019, **11**, 13835–13852.
35 A. O. Govorov, Y. K. Gun'ko, J. M. Slocik, V. A. Gérard, Z. Fan and R. R. Naik, *J. Mater. Chem.*, 2011, **21**, 16806–16818.
36 Y. Zhang, Y. Cui, R. An, X. Liang, Q. Li, H. Wang, H. Wang, Y. Fan, P. Dong, J. Li, K. Cheng, W. Wang, S. Wang, G. Wang, C. Xue and M. Komiyama, *J. Am. Chem. Soc.*, 2019, **141**, 7758–7764.
37 L. Li, Y. Zhang, W. Ma, H. Chen, M. Liu, R. An, B. Cheng and X. Liang, *Nucleic Acids Res.*, 2022, **50**, 684–696.
38 L. Li, R. An and X. Liang, *Molecules*, 2022, **27**, 3706.
39 C. Mao, W. Sun, Z. Shen and N. C. Seeman, *Nature*, 1999, **397**, 144–146.
40 Y. Sun, B. Yang, Y. Hua, Y. Dong, J. Ye, J. Wang, L. Xu and D. Liu, *ChemBioChem*, 2020, **21**, 94–97.
41 B. Yang, B. Zhou, C. Li, X. Li, Z. Shi, Y. Li, C. Zhu, X. Li, Y. Hua, Y. Pan, J. He, T. Cao, Y. Sun, W. Liu, M. Ge, Y. R. Yang, Y. Dong and D. Liu, *Angew. Chem., Int. Ed.*, 2022, **61**, e202202520.
42 H. Dietz, S. M. Douglas and W. M. Shih, *Science*, 2009, **325**, 725–730.
43 S. Sun, Y. Yang, D. Li and J. Zhu, *J. Am. Chem. Soc.*, 2019, **141**, 19524–19528.
44 C. Xie, Z. Chen, K. Chen, Y. Hu, F. Xu and L. Pan, *Nano Lett.*, 2024, **24**, 8696–8701.
45 J. C. Mitchell, J. R. Harris, J. Malo, J. Bath and A. J. Turberfield, *J. Am. Chem. Soc.*, 2004, **126**, 16342–16343.
46 A. M. Maier, W. Bae, D. Schiffels, J. F. Emmerig, M. Schiff and T. Liedl, *ACS Nano*, 2017, **11**, 1301–1306.
47 C. Lin, Y. Ke, Z. Li, J. H. Wang, Y. Liu and H. Yan, *Nano Lett.*, 2009, **9**, 433–436.
48 H. Urata, K. Shinohara, E. Ogura, Y. Ueda and M. Akagi, *J. Am. Chem. Soc.*, 1991, **113**, 8174–8175.
49 H. Urata, E. Ogura, K. Shinohara, Y. Ueda and M. Akagi, *Nucleic Acids Res.*, 1992, **20**, 3325–3332.
50 R. P. Goodman, I. A. Schaap, C. F. Tardin, C. M. Erben, R. M. Berry, C. F. Schmidt and A. J. Turberfield, *Science*, 2005, **310**, 1661–1665.
51 Y. He, M. Su, P. A. Fang, C. Zhang, A. E. Ribbe, W. Jiang and C. Mao, *Angew. Chem., Int. Ed.*, 2010, **49**, 748–751.
52 C. Zhang, W. Wu, X. Li, C. Tian, H. Qian, G. Wang, W. Jiang and C. Mao, *Angew. Chem., Int. Ed.*, 2012, **51**, 7999–8002.
53 D. Han, S. Pal, Y. Liu and H. Yan, *Nat. Nanotechnol.*, 2010, **5**, 712–717.
54 G. Yao, F. Zhang, F. Wang, T. Peng, H. Liu, E. Poppleton, P. Šulc, S. Jiang, L. Liu, C. Gong, X. Jing, X. Liu, L. Wang, Y. Liu, C. Fan and H. Yan, *Nat. Chem.*, 2020, **12**, 1067–1075.
55 G. Zanchetta, F. Giavazzi, M. Nakata, M. Buscaglia, R. Cerbino, N. A. Clark and T. Bellini, *Proc. Natl. Acad. Sci. U. S. A.*, 2010, **107**, 17497–17502.
56 M. Siavashpouri, C. H. Wachauf, M. J. Zakhary, F. Praetorius, H. Dietz and Z. Dogic, *Nat. Mater.*, 2017, **16**, 849–856.
57 M. M. C. Tortora, G. Mishra, D. Prešern and J. P. K. Doye, *Sci. Adv.*, 2020, **6**, eaaw8331.
58 C. Jin, L. Han and S. Che, *Angew. Chem., Int. Ed.*, 2009, **48**, 9268–9272.
59 B. Liu, L. Han and S. Che, *Angew. Chem., Int. Ed.*, 2012, **51**, 923–927.
60 S. Li, Y. Liu, M. He, Y. Yang, S. He, H. Hu, M. Xiong and Y. Lyu, *ACS Nano*, 2024, **18**, 23104–23116.
61 J. F. Schmuck, J. Borggräfe and M. Etzkorn, *Nat. Commun.*, 2024, **15**, 5145.
62 L. Cui, R. Peng, T. Fu, X. Zhang, C. Wu, H. Chen, H. Liang, C. J. Yang and W. Tan, *Anal. Chem.*, 2016, **88**, 1850–1855.
63 W. Ma, H. Kuang, L. Xu, L. Ding, C. Xu, L. Wang and N. A. Kotov, *Nat. Commun.*, 2013, **4**, 2689.
64 A. Kuzyk, R. Schreiber, Z. Fan, G. Pardatscher, E. M. Roller, A. Högele, F. C. Simmel, A. O. Govorov and T. Liedl, *Nature*, 2012, **483**, 311–314.
65 W. Yan, L. Xu, W. Ma, L. Liu, L. Wang, H. Kuang and C. Xu, *Small*, 2014, **10**, 4293–4297.
66 H. Kuang, H. Yin, L. Liu, L. Xu, W. Ma and C. Xu, *ACS Appl. Mater. Interfaces*, 2014, **6**, 364–369.
67 A. Kuzyk, R. Schreiber, H. Zhang, A. O. Govorov, T. Liedl and N. Liu, *Nat. Mater.*, 2014, **13**, 862–866.
68 Y. Huang, M. K. Nguyen, A. K. Natarajan, V. H. Nguyen and A. Kuzyk, *ACS Appl. Mater. Interfaces*, 2018, **10**, 44221–44225.
69 T. Funck, T. Liedl and W. Bae, *Appl. Sci.*, 2019, **9**, 3006.
70 T. Funck, F. Nicoli, A. Kuzyk and T. Liedl, *Angew. Chem., Int. Ed.*, 2018, **57**, 13495–13498.
71 Y. Huang, M. K. Nguyen, V. H. Nguyen, J. Loo, A. J. Lehtonen and A. Kuzyk, *Langmuir*, 2022, **38**, 2954–2960.
72 Y. Huang, J. Ryssy, M. K. Nguyen, J. Loo, S. Hällsten and A. Kuzyk, *Anal. Chem.*, 2022, **94**, 17577–17586.
73 C. Li, T. He, X. Yang, C. Feng, Z. Zhang, J. Zhu, S. Dong, Y. Shi, Z. Wei, H. Jiao, Y. Zhang, H. Liu, Z. Wang and X. Cheng, *Nano Lett.*, 2024, **24**, 9451–9458.

74 M. Sun, L. Xu, J. H. Bahng, H. Kuang, S. Alben, N. A. Kotov and C. Xu, *Nat. Commun.*, 2017, **8**, 1847.
75 L. Xu, Y. Gao, H. Kuang, L. M. Liz-Marzán and C. Xu, *Angew. Chem., Int. Ed.*, 2018, **57**, 10544–10548.
76 W. Zheng, P. Huang, D. Tu, E. Ma, H. Zhu and X. Chen, *Chem. Soc. Rev.*, 2015, **44**, 1379–1415.
77 B. Zhou, B. Shi, D. Jin and X. Liu, *Nat. Nanotechnol.*, 2015, **10**, 924–936.
78 X. Wu, L. Xu, W. Ma, L. Liu, H. Kuang, N. A. Kotov and C. Xu, *Adv. Mater.*, 2016, **28**, 5907–5915.
79 S. Li, L. Xu, W. Ma, X. Wu, M. Sun, H. Kuang, L. Wang, N. A. Kotov and C. Xu, *J. Am. Chem. Soc.*, 2016, **138**, 306–312.
80 F. Liu, N. Li, Y. Shang, Y. Wang, Q. Liu, Z. Ma, Q. Jiang and B. Ding, *Angew. Chem., Int. Ed.*, 2022, **61**, e202114706.
81 Y. Fang, K. Bansal, S. Mostafavi, C. Benoist and D. Mathis, *Nature*, 2024, **628**, 400–407.
82 Y. Lei, J. J. VanPortfliet, Y. F. Chen, J. D. Bryant, Y. Li, D. Fails, S. Torres-Odio, K. B. Ragan, J. Deng, A. Mohan, B. Wang, O. N. Brahms, S. D. Yates, M. Spencer, C. W. Tong, M. W. Bosenberg, L. C. West, G. S. Shadel, T. E. Shutt, J. W. Upton, P. Li and A. P. West, *Cell*, 2023, **186**, 3013–3032.
83 P. R. Marshall, Q. Zhao, X. Li, W. Wei, A. Periyakaruppiah, E. L. Zajaczkowski, L. J. Leighton, S. U. Madugalle, D. Basic, Z. Wang, J. Yin, W. S. Liau, A. Gupte, C. R. Walkley and T. W. Bredy, *Nat. Neurosci.*, 2020, **23**, 718–729.
84 T. Zhang, C. Yin, A. Fedorov, L. Qiao, H. Bao, N. Beknazarov, S. Wang, A. Gautam, R. M. Williams, J. C. Crawford, S. Peri, V. Studitsky, A. A. Beg, P. G. Thomas, C. Walkley, Y. Xu, M. Poptsova, A. Herbert and S. Balachandran, *Nature*, 2022, **606**, 594–602.
85 Z. Wang, D. Zhang, X. Qiu, H. Inuzuka, Y. Xiong, J. Liu, L. Chen, H. Chen, L. Xie, H. Kaniskan, X. Chen, J. Jin and W. Wei, *J. Am. Chem. Soc.*, 2024, **146**, 7584–7593.
86 J. T. Sczepanski and G. F. Joyce, *J. Am. Chem. Soc.*, 2013, **135**, 13290–13293.
87 S. Klussmann, A. Nolte, R. Bald, V. A. Erdmann and J. P. Fürste, *Nat. Biotechnol.*, 1996, **14**, 1112–1115.
88 J. Chen, M. Chen and T. F. Zhu, *Nat. Biotechnol.*, 2022, **40**, 1601–1609.
89 K. Hoehlig, K. W. Johnson, E. Pryazhnikov, C. Maasch, A. Clemens-Smith, W. G. Purschke, S. Vauléon, K. Buchner, F. Jarosch, L. Khiroug, A. Vater and S. Klussmann, *Br. J. Pharmacol.*, 2015, **172**, 3086–3098.
90 T. Denekas, M. Tröltzsch, A. Vater, S. Klussmann and K. Messlinger, *Br. J. Pharmacol.*, 2006, **148**, 536–543.
91 B. Wlotzka, S. Leva, B. Eschgfäller, J. Burmeister, F. Kleinjung, C. Kaduk, P. Muhn, H. Hess-Stumpp and S. Klussmann, *Proc. Natl. Acad. Sci. U. S. A.*, 2002, **99**, 8898–8902.
92 C. Maasch, A. Vater, K. Buchner, W. G. Purschke, D. Eulberg, S. Vonhoff and S. Klussmann, *J. Biol. Chem.*, 2010, **285**, 40012–40018.
93 W. G. Purschke, D. Eulberg, K. Buchner, S. Vonhoff and S. Klussmann, *Proc. Natl. Acad. Sci. U. S. A.*, 2006, **103**, 5173–5178.
94 K. Hoehlig, C. Maasch, N. Shushakova, K. Buchner, M. Huber-Lang, W. G. Purschke, A. Vater and S. Klussmann, *Mol. Ther.*, 2013, **21**, 2236–2246.
95 J. Hoellenriegel, D. Zboralski, C. Maasch, N. Y. Rosin, W. G. Wierda, M. J. Keating, A. Kruschinski and J. A. Burger, *Blood*, 2014, **123**, 1032–1039.
96 M. Gobbi, M. Steurer, F. Caligaris-Cappio, M. Montillo, A. Janssens, L. Trentin, T. Dümmler, S. Zöllner, S. Zeitler, K. Riecke and A. Kruschinski, *Blood*, 2013, **122**, 1635.
97 D. Möckel, M. Bartneck, P. Niemietz, M. Wagner, J. Ehling, E. Rama, M. Weiler, F. Gremse, D. Eulberg, R. Pola, M. Pechar, T. Etrych, G. Storm, F. Kiessling, F. Tacke and T. Lammers, *J. Controlled Release*, 2024, **365**, 358–368.
98 J. Menne, D. Eulberg, D. Beyer, M. Baumann, F. Saudek, Z. Valkusz, A. Więcek and H. Haller, *Nephrol., Dial., Transplant.*, 2017, **32**, 307–315.
99 K. Riecke, S. Zöllner, M. Boyce, B. vanHecke, S. Vauléon, L. Summo, C. M. Laarakkers, D. W. Swinkels and F. Schwöbel, *Am. J. Hematol.*, 2013, **88**, E225–E226.
100 S. Fujimori, K. Shudo and Y. Hashimoto, *J. Am. Chem. Soc.*, 1990, **112**, 7436–7438.
101 D. J. Anderson, R. J. Reischer, A. J. Taylor and W. J. Wechter, *Nucleosides, Nucleotides Nucleic Acids*, 1984, **3**, 499–512.
102 P. L. Tran, R. Moriyama, A. Maruyama, B. Rayner and J. L. Mergny, *Chem. Commun.*, 2011, **47**, 5437–5439.
103 K. R. Kim, T. Lee, B. S. Kim and D. R. Ahn, *Chem. Sci.*, 2015, **6**, 2122.
104 K. R. Kim, H. Y. Kim, Y. D. Lee, J. S. Ha, J. H. Kang, H. Jeong, D. Bang, Y. T. Ko, S. Kim, H. Lee and D. R. Ahn, *J. Controlled Release*, 2016, **243**, 121–131.
105 J. H. Kang, K. R. Kim, H. Lee, D. R. Ahn and Y. T. Ko, *Colloids Surf., B*, 2017, **157**, 424–431.
106 K. R. Kim, D. Hwang, J. Kim, C. Y. Lee, W. Lee, D. S. Yoon, D. Shin, S. J. Min, I. C. Kwon, H. S. Chung and D. R. Ahn, *J. Controlled Release*, 2018, **280**, 1–10.
107 H. B. D. Thai, K. R. Kim, K. T. Hong, T. Voitsitskyi, J. S. Lee, C. Mao and D. R. Ahn, *ACS Cent. Sci.*, 2020, **6**, 2250–2258.
108 L. Xu, X. Wang, W. Wang, M. Sun, W. J. Choi, J. Y. Kim, C. Hao, S. Li, A. Qu, M. Lu, X. Wu, F. M. Colombari, W. R. Gomes, A. L. Blanco, A. F. de Moura, X. Guo, H. Kuang, N. A. Kotov and C. Xu, *Nature*, 2022, **601**, 366–373.

